

Design and Implementation of a Sliding Mode Control based Pitch Controller for a Variable Pitch Wind Turbine

Van Roy Tran

Energy Technology, OES10-7-E20, 2020-12

Master Project



Preface

This report is written and produced by the members of OES10-7-E20 in cooperation with Aalborg University Esbjerg. The report is written as an Master project during Fall 2020 and is inspired by previous work of former students.

This project acknowledge the guidance of the supervisor, Associate Professor Mohsen N. Soltani for the support throughout this study.

The report is organized as follows. In chapter 1 an introduction to the study is given and the experimental setup is introduced. Chapter 2 focuses on the modelling of the wind energy system, which is used for the design of the Sliding Mode Controller in chapter 3. In chapter 4 the focus is on the implementation of the control scheme in MATLAB Simulink and then validation of the proposed control scheme. Finally, when the controller has been validated, simulation results of performance of the controller is investigated in chapter 5. Chapter 6 and Chapter 7 discusses the results of the study and concludes the report.

In the report the references is marked with a number inside a square bracket chronologically throughout the report. The references consists of articles, technical reports, books and websites and is listed in the Bibliography in the end of the report. The equation in the report is also marked with a number to the far right, tables and figures is numbered either above or below them including a short description.

Aalborg University Esbjerg, Dec 1, 2020



Van Roy Tran

vtran15@student.aau.dk



Energy Technology
Aalborg University Esbjerg
<http://www.aau.dk>

AALBORG UNIVERSITY

STUDENT REPORT

Title:

Design and Implementation of a Sliding Mode Control based Pitch Controller for a Variable Pitch Wind Turbine

Theme:

Non-linear Sliding Mode Control

Project Period:

Fall Semester 2020

Project Group:

OES10-7-F20

Participants:

Van Roy Tran

Supervisor:

Mohsen Soltani

Copies: 1

Page Numbers: 40

Date of Completion:

May 29, 2019

Abstract:

This report focuses on the implementation of a non-linear control scheme for a variable pitch wind turbine operating above rated wind speed. For this purpose a Sliding Mode Control based pitch controller is designed by deriving a control law based on the dynamic equation of the system.

These control laws are derived based on Lyapunov Function Approach and then implemented in the developed Simulink model of the wind turbine. To validate the proposed control laws, simulation with real-life wind disturbance data are used. The simulation results showed that a pitch controller based on Integral Sliding Mode Control is capable of dealing with the rapid changes in the wind speed and also tracking the reference rotational velocity.

The content of this report is freely available, but publication (with reference) may only be pursued due to agreement with the author.

Contents

Preface	iii
1 Introduction	1
1.1 Experimental setup	2
1.1.1 Wind turbine	3
2 Modeling	5
2.1 Aerodynamic Rotor model	6
2.2 Drive-Train model	8
2.3 State-space representation	9
3 Control Scheme	11
3.1 Control region of wind turbine	11
3.2 Sliding Mode Control	12
3.2.1 Design of SMC	13
3.2.2 Design of control law	14
3.2.3 Chattering	16
3.3 Integral Sliding Mode Control	17
4 Implementation of ISMC and SMC scheme	19
4.1 SMC and ISMC Simulink model	19
4.1.1 Control parameters	21
4.1.2 Operating conditions	21
4.1.3 Comparison of ISMC and SMC	23
5 Simulation and validation	25
5.1 Wind disturbance simulation results	25
5.2 Comparison with PI control	27
6 Discussion	29
7 Conclusion	31

Bibliography	33
A Appendix	35
A.1 MATLAB SMC Code	35
A.2 MATLAB ISMC Code	36
A.3 Non-linear subsystem:Rotor model	37
A.4 Non-linear subsystem:Drive-train model	38
A.5 MATLAB PI Code	39
A.6 Non-linear system with PI control scheme	40

Chapter 1

Introduction

In recent years, wind energy has become one of the most prominent competitors in the field of renewable energies. Its reputation of being a clean and safe renewable energy source that is inexhaustible makes it very attractive.

However, the conversion from the energy in the wind into electrical energy in a wind energy system can be very challenging due to its non-linear models and input variations. The uncertainties and randomness that is naturally introduced in such system makes the control of the wind turbine especially troublesome. Due to these non-linearities, non-linear control are becoming more prevalent compared to traditional control methods, such as the PID control scheme. Even though, the PID control scheme is widely used, it has its limitations when it comes to the model uncertainties.

The realization of a Sliding Mode Control (SMC) scheme in a wind energy system has been proven in several studies ([1] [2] [3]). These studies have shown that the SMC scheme are robust when it comes parameter variations and dealing with external disturbances. Also, their capability of stabilizing the system states to a specified control target using rather simple designs makes them very intriguing.

The objective of this study aims to provide a non-linear SMC based pitch controller for a wind energy system located on a experimental floating platform. The controller should be able to deal with the parameter changes and external disturbance that involves in a wind energy system.

However, first, an dynamic model for the wind turbine have to be derived and a MATLAB Simulink model should be developed since it lays the foundation for the control laws. In the end, the controller should be validated through simulations and tested under condition that resembles real-life conditions.

1.1 Experimental setup

The experimental setup used for this project is shown in figure 1.1. The setup primarily consists of a wind generator placed in the front, a huge water tank with a wave generator, and in the middle of water tank a Floating Offshore Wind Turbine (FOWT) with a Tension Leg Platform (TLP) foundation.

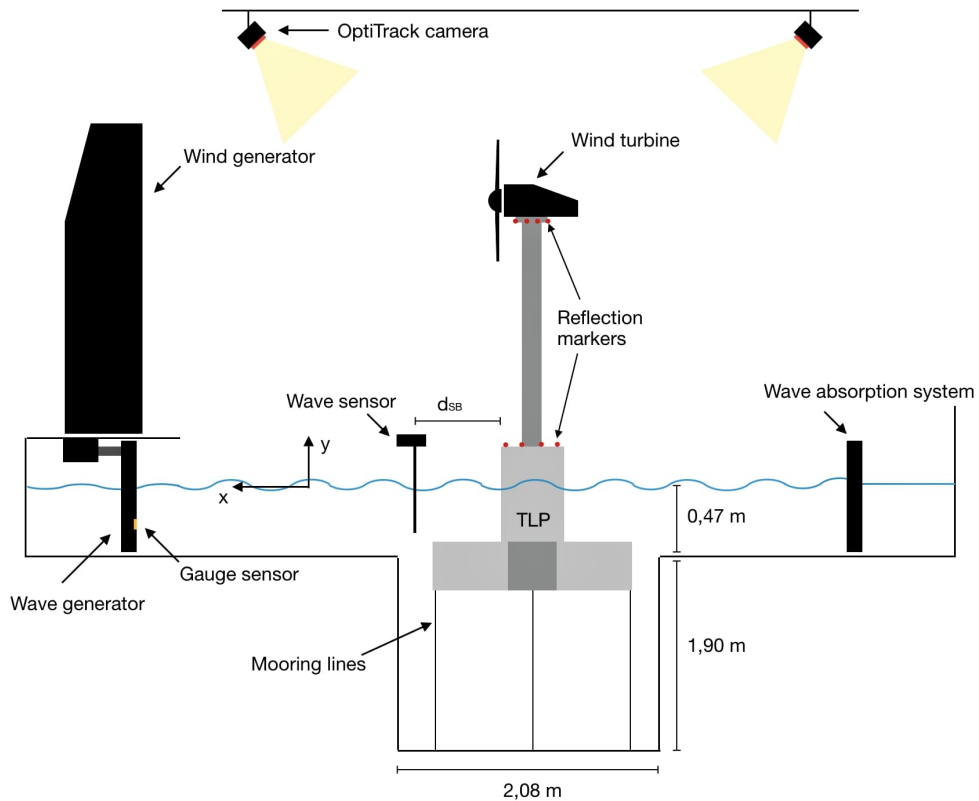


Figure 1.1: Overview of the entire experimental setup on AAU campus[oes_rikke]

The wind generator in front of the FOWT consists of seven large fans placed in a honeycomb pattern. From a control panel, the number of fans and their velocity can be controlled, such that a wind speed ranging from 0 m/s to 8.5 m/s is generated.

Above the experimental setup, 8 OptiTrack cameras are installed. These cameras are used to measure the displacement, velocity, and acceleration of the FOWT by tracking reflective markers placed on the top and bottom of the FOWT.

As the focus in this project is only on the aerodynamic part of the setup, the hydrodynamic part will not be covered.

1.1.1 Wind turbine

The wind turbine itself, is a 1:35 scaled version of the 5 MW NREL reference turbine built by former students at Aalborg University Esbjerg [4]. This turbine is not a real operating wind turbine, but it is constructed as theoretical representation of a three bladed variable speed variable pitch wind turbine used for academic study purposes involving offshore wind technology.

In figure 1.2 the FOWT in front of the wind generator is shown.



Figure 1.2: The FOWT in front of the wind generator seen from the back

As the FOWT and the entire experimental setup has been used in many other projects, the foundation of this project will be built on the work of others.

Chapter 2

Modeling

Before going in depth with the SMC, a thorough analysis of the system and its subsystem is required. The development of the dynamic models of the entire FOWT have as mentioned already been investigated in previous works [5] [4]. However, for the development of the SMC based pitch controller, the focus will be only on the top part of the FOWT. A general overview of the top part of the wind turbine and its subsystem are shown in figure 2.1

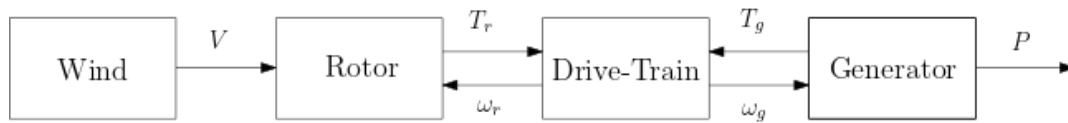


Figure 2.1: Block diagram for the subsystems of the wind turbine

The conversion from an input wind speed to generated power is illustrated in the block diagram of the different subsystems. These subsystem each have their inputs and outputs and in the following chapter, the dynamic equations of these will be derived.

2.1 Aerodynamic Rotor model

The relation between the available power in the wind and the mechanical power captured by the wind turbine is calculated by equation 2.1

$$P = \frac{1}{2}\rho AC_p(\lambda, \beta)V^3 \quad (2.1)$$

where ρ is the density of the wind, A is the area swept by the wind turbine blades, and V is the wind speed. C_p is the power coefficient of the wind turbine and shows the efficiency of a wind turbine to convert the available power in the wind to electrical power.

As shown in equation 2.1 the power coefficient is a non-linear function which depends on the tip speed ratio (TSR), λ and the pitch angle, β . The power coefficient is a unique value that depends on its operating conditions and the aerodynamic forces surrounding the rotor blade. To model the power coefficient it will be referred to the findings in [1] which present the following equation for the power coefficient as

$$C_p(\lambda, \beta) = k_5(k_1\gamma + k_2 * \beta + k_3)e^{k_4\gamma} \quad (2.2)$$

$$\gamma = \left(\frac{1}{\lambda + 0.08\beta} - \frac{0.035}{\beta^3 + 1} \right)$$

where the coefficient k_i is a constant that depends on the aerodynamic performance of the blade design. The coefficients are given as:

$$k_1 = 7.022, \quad k_2 = -0.04176, \quad k_3 = -0,3863, \quad k_4 = -14.52, \quad k_5 = 6.909 \quad (2.3)$$

These results are based on the 5 MW NREL reference wind turbine and therefore also applicable in this study. The non-linearity relationship between C_p and β , λ is illustrated in figure 2.2.

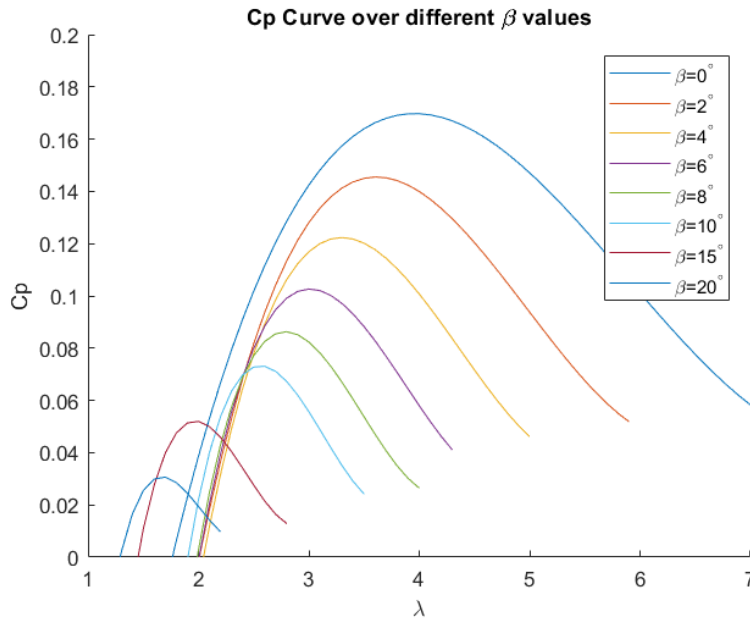


Figure 2.2: The C_p curve for different pitch angles and tip speed ratios [6]

The C_p curve shows that for a given pitch angle, there is a unique power coefficient which corresponds to maximum power extraction, $C_{p_{max}}$.

The tip speed ratio is generally defined as the ratio between the linear velocity of the blade tip and the wind speed and is calculated as:

$$\lambda = \frac{\omega_r R}{V} \quad (2.4)$$

where ω_r is the rotor speed and R is the radius of the rotor.

The aerodynamic torque, τ of the rotor can be expressed in terms of the rotor speed and the mechanical power as:

$$T_r = \frac{P}{\omega_r} \quad (2.5)$$

which can be rewritten as:

$$T_r = \frac{\frac{1}{2}\rho A C_p(\lambda, \beta) V^3}{\omega_r} \quad (2.6)$$

2.2 Drive-Train model

The drive-train on a wind turbine is the component that is responsible for transferring the power which is captured by the rotor from the wind onto the generator side. The main components of this particular drive-train are the low speed shaft, which is connected to the rotor, the high speed shaft within the generator, and a gearbox which links the components. An illustration of the entire drive-train on the experimental setup is shown on figure .

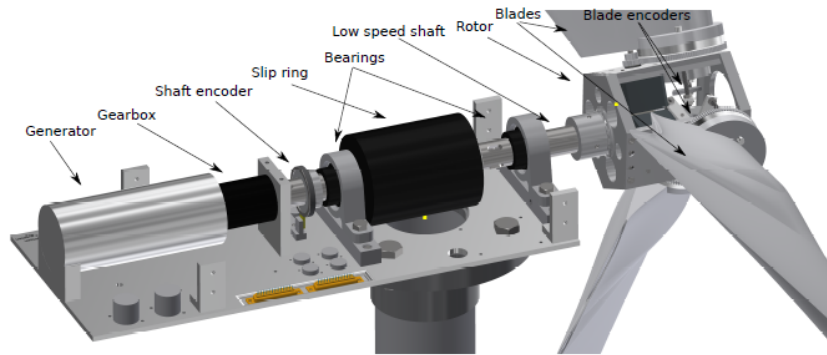


Figure 2.3: The components of the drive-train on the experimental setup [10_semester]

The dynamic equation for the drive-train can be derived from the relationship between the different torques from the generator and the rotor as shown in equation 2.7

$$T_r - T_g N_g = J_{dt} \dot{\omega}_r + B_{dt} \omega_r \quad (2.7)$$

where T_r is the low speed shaft rotor torque, T_g is the high speed shaft generator torque, J_{dt} is the moment of inertia of the rotor blades, B_{dt} is the viscous friction, ω_r is the rotor speed and N_g is the gearbox ratio.

According to the dynamic equation of the drive-train, to accelerate the rotor the torque of the rotor must be larger than the torque of the generator. The opposite also applies for deceleration of the rotor, which is the rotor torque must be less than the generator torque. This should be kept in mind as it lays the foundation of the control principle of the pitch controller, which is further explained in the upcoming chapter.

2.3 State-space representation

From the derived equations in the latter sections the wind turbine model can be rewritten in the following state-space form. [6]

$$\begin{aligned} \dot{x} &= Ax + Bu + Ed \\ y &= Cx \end{aligned} \quad (2.8)$$

where the state-space variables are given as

$$x = [\omega], \quad u = [\beta], \quad d = [V], \quad y = [\omega] \quad (2.9)$$

In the model the wind speed, V is considered as a disturbance input and it is described by the vector, d .

Considering the drive-train model in equation 2.7, it can be rewritten as a function of the rotational acceleration as

$$\dot{\omega} = \frac{\frac{1}{2}\rho AV^3 C_p(\lambda, \beta)}{J\omega} - \frac{T_g}{J} - \frac{B_{dt}\omega}{J} \quad (2.10)$$

As the rotational acceleration relates to the three variables V, β, ω , equation 2.10 can be shorten as

$$\dot{\omega} = f(\omega, \beta, V) \quad (2.11)$$

Due to the non-linear parameter C_p , equation 2.10 has to be linearized with respect to the three variables V, β, ω . For this Taylor expansion is used, where only the first order terms are considered. [6] The following expression is then obtained for the wind turbine as

$$\Delta f = \left. \frac{\partial f}{\partial \omega} \right|_{f_0} \Delta \omega + \left. \frac{\partial f}{\partial V} \right|_{f_0} \Delta V + \left. \frac{\partial f}{\partial \beta} \right|_{f_0} \Delta \beta \quad (2.12)$$

Here the Δ values denotes the difference between the actual values and the reference values. When substituting the expression for the linearized terms in equation 2.12 into the state-space matrices, the model can be rewritten as

$$\Delta \dot{x} = \left[\frac{\partial f}{\partial \omega} \right] \Delta x + \left[\frac{\partial f}{\partial \beta} \right] \Delta u + \left[\frac{\partial f}{\partial V} \right] \Delta d \quad (2.13)$$

Where the A , B , and E matrices are given as

$$A = \left[\frac{\partial f}{\partial \omega} \right], \quad B = \left[\frac{\partial f}{\partial \beta} \right], \quad E = \left[\frac{\partial f}{\partial V} \right] \quad (2.14)$$

Finally, by substituting equation 2.10 in the different matrices an final expression for the system is given as

$$\begin{aligned}
 \mathbf{A} &= \left[-\frac{\frac{1}{2}\rho AV^3 C_p(\lambda, \beta)}{J\omega^2} + \frac{\frac{1}{2}\rho AV^3}{J\omega} \cdot \frac{\partial C_p(\lambda, \beta)}{\partial \lambda} \cdot \frac{R}{V} \right] \\
 \mathbf{B} &= \left[\frac{\frac{1}{2}\rho AV^3}{J\omega} \cdot \frac{\partial C_p(\lambda, \beta)}{\partial \beta} \right] \\
 \mathbf{E} &= \left[\frac{\frac{3}{2}\rho AV^2 C_p(\lambda, \beta)}{J\omega} - \frac{\frac{1}{2}\rho AVR}{J} \cdot \frac{\partial C_p(\lambda, \beta)}{\partial \lambda} \right]
 \end{aligned} \tag{2.15}$$

Chapter 3

Control Scheme

In this chapter, the control objectives in a wind energy system and a Sliding Mode Controller is introduced and a design of the SMC based pitch controller is proposed.

3.1 Control region of wind turbine

As mentioned, the reference wind turbine used in this study is considered as a variable speed variable pitch wind turbine. The control regions of a variable speed variable pitch wind turbine can be divided into four regions according to the cut-in wind speed, rated wind speed, and cut-out wind speed as shown in figure 3.1.

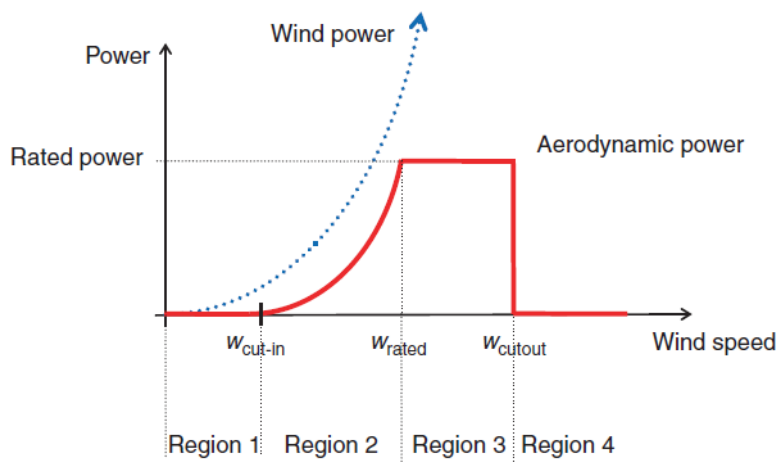


Figure 3.1: Operating regions of a variable speed variable pitch wind turbine [6]

In region I, the wind speed is below the cut-in wind speed and here it is too low for the turbine to generate power due to the inertia of the rotating system.

In region II, the wind speed is in between the cut-in wind speed and the rated wind speed, here, the output power of the turbine slowly increases until it reaches the rated wind speed. As the wind speed increases in this region the control strategy is to ensure Maximum Power Point Tracking (MPPT), which means that an optimum TSR is required to optimize the power extraction.

In region III, the wind speed is higher than the rated wind speed and lower than the cut-out wind speed. To ensure that the mechanical and electrical parts are working in safe operation, a pitch controller is used to adjust the pitch angle and stabilize the power output at its rated power output.

In region IV, the wind speed is higher than the cut-out wind speed and to prevent any damage to the wind turbine it shuts down.[7]

As the primary objective in this project is the design of a SMC based pitch controller, region III will be the focus area. In region III, high wind speeds is considered and the objective of the control will be to maintain the power output at a rated value. As maintaining the power output corresponds to maintaining the rotational velocity to a fixed value, the pitch angle, β is used as the control input, since a change in the pitch angle corresponds to a change in the aerodynamic force affecting the blades.

3.2 Sliding Mode Control

Sliding Mode Control (SMC) is a non-linear control method and is a particular type of variable structure control that alters the structure of a system according to the development of its states. The idea behind SMC is to apply different feedback laws to a system which forces its trajectories on to a predetermined surface in state space. Some of the main advantages of SMC includes robustness, finite-time convergence, rapid response, and simple control design. [8]

SMC is often split up in two principal control phases: The first one being the reaching phase where the controller forces the system states onto a particular sliding surface. Once the sliding surface has been reached, it then switches to its second phase, the sliding phase, where the system states are forced to slide along the sliding surface and remain there afterwards. Hence, the design of the controller involves two steps, the design of the sliding surface and appropriate selection of control laws to ensure that the above mentioned tasks can be achieved.

In figure 3.2, the behavior of the system states using sliding mode control is shown.

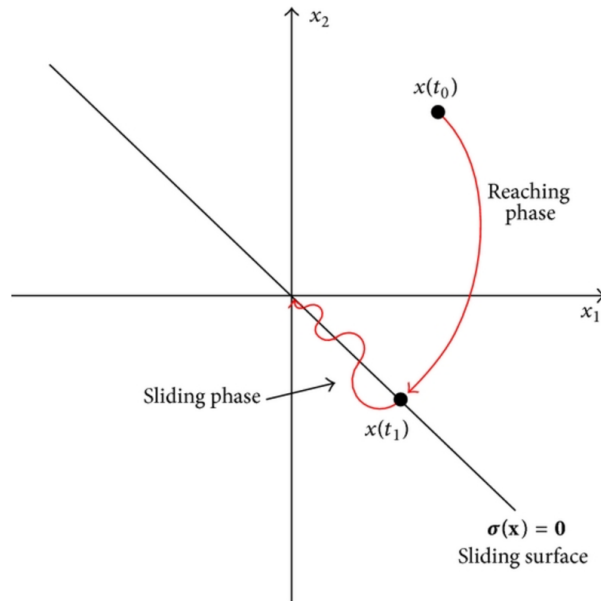


Figure 3.2: The system states in sliding mode control [9].

3.2.1 Design of SMC

In the designing process of a SMC, a switching function, σ is defined as

$$\sigma(x) : R^n \rightarrow R^m \quad (3.1)$$

where n represents the number of states and m the number of input signals. The introduction of the switching function involves indexing a desired or designed dynamics based on the system states into a new state variable. [10]

In this case, it is associated with the error signal and is defined as

$$\epsilon = \omega - \omega_{ref} \quad (3.2)$$

where ω_{ref} is the reference rotational velocity.

The switching function represents the dynamics that the system is forced to adjust to by a certain control law, u . The purpose of the switching function is to describe a certain "distance" the states are from the sliding surface, where $\sigma(x) \neq 0$ means that a state is outside of the sliding surface and $\sigma(x) = 0$ that the states are on the surface. [11]

Since the sliding surface determines the dynamics of the plant in the sliding mode, the selection of an appropriate sliding surface is very important. To ensure that the value of the switching function is driven to zero $\sigma(x) = 0$, the following sliding surface is proposed as

$$\sigma = \epsilon = \omega - \omega_{ref} \quad (3.3)$$

From equation 3.3 it is obvious that if σ is driven to zero then the rotational velocity coincides with the desired reference rotational velocity which means that error signal is also driven to zero.

3.2.2 Design of control law

The next step in the design process is the design of a control law to ensure that $\sigma(x)$ is driven to zero in finite time and remain there afterwards. The design of the control law, u is composed of two elements as shown in equation 3.4.

$$u(t) = u_c(t) + u_{eq}(t) \quad (3.4)$$

$u_c(t)$ is the corrective control, responsible for reaching the sliding surface and $u_{eq}(t)$ is the equivalent control, responsible for remaining on the surface once it has been reached.

Different methods can be used to derive these control laws, however, in this project the Lyapunov Function Approach will be considered.

For the Lyapunov Function Approach a Lyapunov function candidate is selected as:

$$V = \frac{1}{2}\sigma^2 \quad (3.5)$$

According to the transversal condition in [8], *"the existence of a sliding regime on $\sigma = 0$ entitles the opposite growth of the sliding surface coordinate function σ on a sufficiently large open vicinity. If x is located in such a vicinity, so that $\sigma > 0$, the time derivative $\dot{\sigma}$ must be negative and, hence σ decreases. On the other hand if x is such that $\sigma < 0$, the time derivative $\dot{\sigma}$ must be positive and σ increases towards its zero value"*

In other words, the following conditions must be satisfied for the Lyapunov function: First equation 3.5 must be positive definite and secondly the derivative of the candidate function must be negative definite as shown in the equation 3.6. [11]

$$\begin{aligned} V &= \frac{1}{2}\sigma^2 > 0 \\ \dot{V} &= \dot{\sigma}\sigma < 0 \end{aligned} \quad (3.6)$$

Equivalent control

Assuming that an appropriate control law manage to drive the state variable x to zero, the equivalent control is then responsible of maintaining the evolution of the states according to the defined sliding surface. In other words, sliding mode occurs and $\sigma = \dot{\sigma} = 0$. Supposing that the error signal and its derivative is given as $x_1 = \omega - \omega_{ref}$ and $x_2 = \dot{x}_1 = \dot{\omega}$, the sliding surface and its derivative can be expressed as

$$\begin{aligned}\sigma &= x_1 \\ \dot{\sigma} &= \dot{x}_1 = x_2\end{aligned}\quad (3.7)$$

The equivalent control law, u_{eq} on the sliding mode can then be found by solving the derivative of the sliding surface equal 0 ($\dot{\sigma} = 0$). By using the formulation obtained from the Taylor expansion in equation 2.10, 2.11, and 2.14 the following expression is obtained.

$$\dot{\sigma} = \mathbf{A}\Delta\omega + \mathbf{B}\Delta\beta + \mathbf{E}\Delta V \quad (3.8)$$

where $\Delta\omega = \omega - \omega_{ref} = x_1$, $\Delta\beta = \beta - \beta_{ref}$, and $\Delta V = V - V_{ref}$. By isolating β , which is the control input, in equation 3.8 a control law for the equivalent control is obtained as shown in equation 3.9.

$$u_{eq} = \beta_{ref} - \mathbf{B}^{-1}(\mathbf{A}x_1 + \mathbf{E}V - V_{ref}) \quad (3.9)$$

Corrective control

For the corrective control, u_c the main objective is to make sure that the sliding surface is reached and that the criteria for stability of the Lyapunov function is satisfied. Therefore, the following control law is proposed.

$$u_c = -K \text{sign}(\sigma) \quad (3.10)$$

where K is the control gain and the $\text{sign}(\sigma)$ is a sign function which is defined as

$$\text{sign}(\sigma) = \begin{cases} 1, & \text{if } \sigma > 0. \\ -1, & \text{if } \sigma < 0. \end{cases} \quad (3.11)$$

When using equation 3.10 we ensure that σ goes to zero in finite time.

Lyapunov Stability

Now we want to check if the Lyapunov stability criterion have been met by the proposed control laws. Using the Lyapunov candidate function from equation 3.6 we get

$$\begin{aligned}\dot{V} &= \sigma\dot{\sigma} \\ \dot{V} &= \sigma(x_2) = \sigma(\mathbf{A}x_1 + \mathbf{B}(\beta - \beta_{ref})\beta + \mathbf{E}(V - V_{ref}))\end{aligned}\quad (3.12)$$

And by insetting the terms for both control law, the equivalent and corrective control in equation 3.12

$$\dot{V} = \sigma(\mathbf{A}x_1 + \mathbf{B}[\beta_{ref} - \mathbf{B}^{-1}(\mathbf{A}x_1 + \mathbf{E}V - V_{ref})] - \beta_{ref} + \mathbf{E}V - V_{ref}) \quad (3.13)$$

It is noticeable that most of the terms cancels each other out and the remaining is therefore

$$\dot{V} = \sigma(-k \text{sign}(\sigma)) \quad (3.14)$$

Examining this expression, we see that when σ is positive, \dot{V} is negative due to the negative control gain, and when σ is negative, \dot{V} is also negative. Thus, when $\sigma \neq 0$, \dot{V} is negative definite which means that the stability criterion has been met.

Finally, it has then been proven that a control law for both the corrective and equivalent control is given for the wind turbine model as shown in equation 3.15

$$u = \beta_{ref} - (\mathbf{B}^{-1}(\mathbf{A}\Delta\omega + \mathbf{E}\Delta V) - K \text{sign}(\sigma)) \quad (3.15)$$

This control law forces the system trajectory to zero in finite amount of time and makes sure that they remain there.

3.2.3 Chattering

One of the major drawbacks of SMC is the chattering phenomenon. Chattering is high frequency oscillations which occurs in vicinity of the sliding surface because of high frequency switching of the input. The chattering phenomenon is very undesirable as it potentially wears down the mechanical components in a system, especially actuators.

To avoid the chattering phenomenon in this project, a boundary layer with a certain thickness is introduced around the sliding surface. This is represented by replacing the sign function with a saturation function instead in equation 3.10. The saturation function is defined as shown in equation 3.16. [12]

$$\text{sat}(\sigma) = \begin{cases} \frac{1}{\psi}\sigma, & \text{if } \sigma < \delta. \\ \text{sign}(\sigma), & \text{Otherwise.} \end{cases} \quad (3.16)$$

where ψ is the thickness of the designed boundary layer.

3.3 Integral Sliding Mode Control

Another drawback of SMC is the occurrence of steady state error, in particular for variable speed wind turbines. To overcome the steady state error, an integral action on the sliding surface can be included. This method is often referred to as Integral Sliding Mode Control (ISMC). By adding a integral action to the conventional SMC a new sliding surface can be expressed as

$$\sigma(t) = \epsilon(t) + K_i \int_0^{\infty} \epsilon(t) dt \quad (3.17)$$

and its derivative as

$$\dot{\sigma}(t) = \dot{\epsilon}(t) + K_i \epsilon(t) \quad (3.18)$$

By substituting equation 3.17 and 3.18 in equation 3.8, a new expression for the equivalent control law is obtained.

$$u_{eq1} = \beta_{ref} - \mathbf{B}^{-1}(\mathbf{A}x_1 + \mathbf{E}V - V_{ref}) + K_i \epsilon \quad (3.19)$$

As the corrective control law remains the same, a final control law for the control scheme can be written as shown in equation 3.20.

$$u = \beta_{ref} - (\mathbf{B}^{-1}(\mathbf{A}\Delta\omega + \mathbf{E}\Delta V) + K_i \epsilon - K \text{sat}(\sigma)) \quad (3.20)$$

Chapter 4

Implementation of ISMC and SMC scheme

In this chapter, the mathematical models and the proposed control scheme is implemented in a MATLAB Simulink model and validated.

4.1 SMC and ISMC Simulink model

The non-linear Simulink model of the wind turbine with the implemented SMC scheme is shown in figure 4.1.

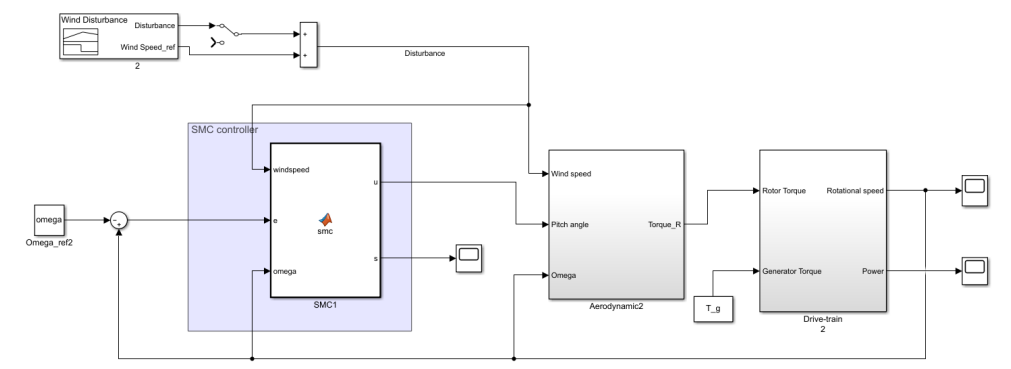


Figure 4.1: The Simulink model of the wind turbine with the implemented SMC scheme

The non-linear Simulink model of the wind turbine with the implemented ISMC scheme is shown in figure 4.2.

4.1.1 Control parameters

As shown in the previous chapter, a few control parameters have to be determined for ISMC scheme. When determining an appropriate control gain, K for the controller, it is usually a trade-off of different characteristics. When the gain is increased, the time required to reach the sliding surface can be reduced, however, increasing it too much may lead to saturation in the actuators and also cause chattering to the control input. By choosing a lower control gain the error in tracking can be reduced, however, risk that it takes a long time to reach the reference value. In this project the requirements for the controller is to first of all, quickly compensate for the disturbance input, which is the wind speed. The reason it has to quickly compensate for the wind speed, is that in real life the wind can change very rapidly and therefore a fast controller is needed to compensate for this. Sensitivity, however, can also be a huge problem, if the control gain is too high it becomes very sensitive and therefore overcompensate for e.g. small gusts of wind.

In this project a trial and error tuning method have been used for the determination of the control parameters. These are shown in table 4.2.

Table 4.2: Determined control parameters

Control parameters	
Control gain, K	75
Boundary layer thickness, ψ	1
Integral gain, K_i	6

4.1.2 Operating conditions

As mentioned in the very first chapter, the experimental wind turbine is a scaled version of the 5 MW NREL reference turbine and its parameters have therefore also been scaled, accordingly. In previous work, made in [5] and [13], the turbine parameters have been scaled to fit the actual experimental setup while still maintaining the dynamic response of the NREL reference turbine.

In figure 4.3, the scaled rotational velocity are shown for both the full-scale and scaled model.

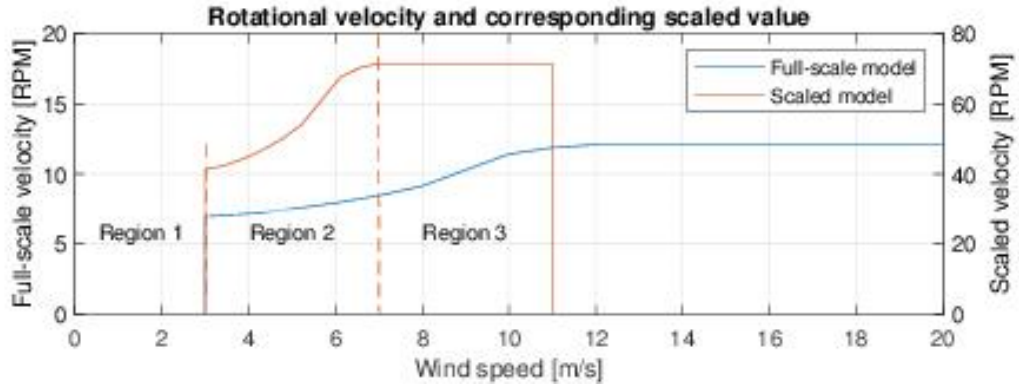


Figure 4.3: The scaled rotational velocity compared to the full-scale NREL turbine rotational velocity[13]

The operating points for the ISMC scheme is given from this scaled model. The beginning of region III occurs at a wind speed of $7m/s$ and it is at this wind speed the pitch controller should start operating. Also, at this wind speed the scaled rotational velocity is at $7.4875rad/s$ and this will be the reference rotational velocity for the controller.

In table 4.3 the operating points for the control scheme is listed.

Table 4.3: The reference value for the pitch control system.

Parameter Name	Symbol	Numerical	Unit
Reference wind speed	V_{ref}	7	m/s
Reference rotational velocity	ω_{ref}	7.4875	rad/s
Reference pitch angle	β_{ref}	15.25	degrees
Reference TSR	λ_{ref}	1.125	
Reference Cp	$C_{p,ref}$	0.0281	
Reference rotor torque	$T_{r,ref}$	3.041	kN·m

4.1.3 Comparison of ISMC and SMC

To examine the differences between the ISMC and the SMC, a small disturbance input is introduced to both system. The result of the simulation is shown in figure 4.4.

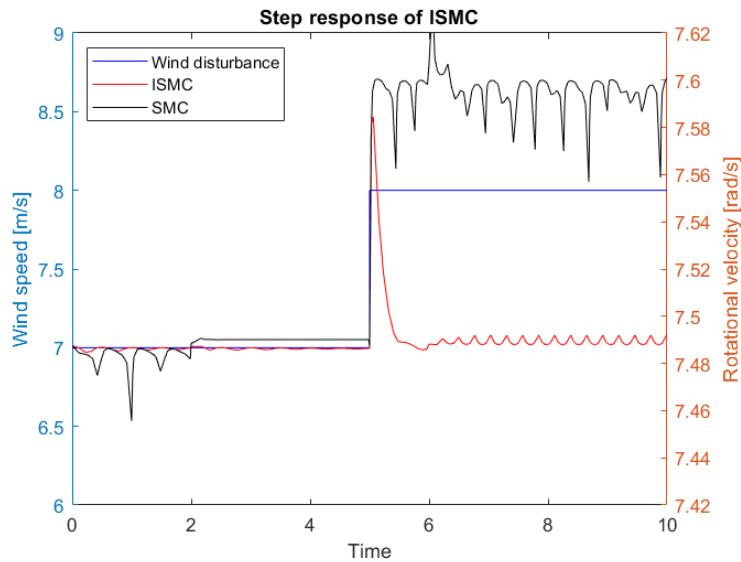


Figure 4.4: The rotational velocity of both control schemes.

As mentioned in the previous chapter, by using a conventional SMC the occurrence of steady state error is shown in the simulation. Even though the SMC scheme quickly responds to the disturbance input, it obviously has a steady state error. The ISMC on the other hand does not encounter this problem, by including the integral part in the controller it has been eliminated.

From these results, it can be concluded that the proposed SMC scheme is not suitable for this particular system, however, the ISMC showed promising results and we will only move along with this scheme for the rest of the report.

Chapter 5

Simulation and validation

In this chapter, an analysis of the ISMC scheme is conducted using wind data profiles that are reminiscent of real life wind behavior. In addition, a comparison between the performance of the classic PI control scheme and the ISMC scheme is examined.

5.1 Wind disturbance simulation results

Since the wind in real life can be very uncertain and unpredictable, examining the performance of the ISMC to real wind data disturbance input is important to investigate. The wind speed data used in the simulations are shown in 5.1.

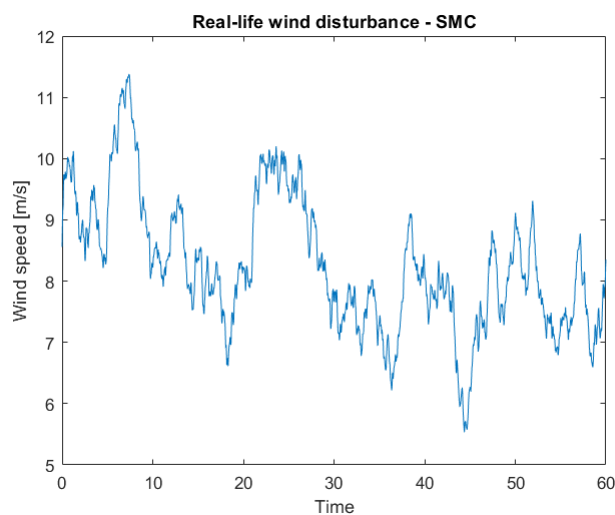


Figure 5.1: Estimation of rotor effective wind speed from [14]

The wind data has a mean wind speed of 7.83 m/s and a maximum deviation from

the mean value of around 2.8 m/s . [15]

The results of the simulations are shown in figure 5.2 where the rotational velocity and pitch angle are shown together with the wind disturbance.

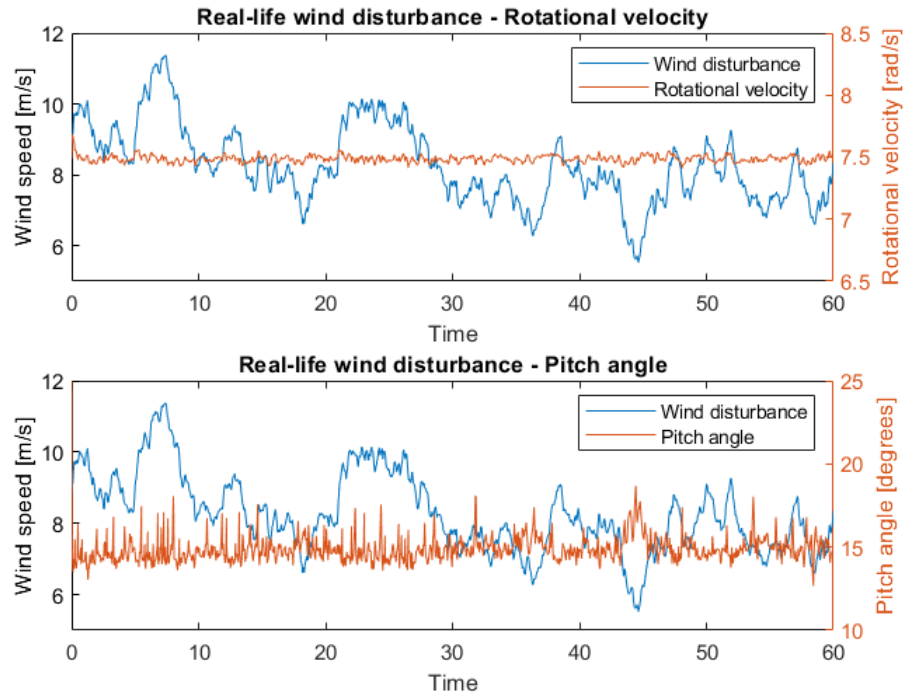


Figure 5.2: Influence of wind disturbance on both the rotational velocity and pitch angle of the ISMC

The simulation results in figure 5.2 shows that the rotational velocity remains constant around the reference value, meaning that there is no steady state error. Even with rapid changes in the wind speed, the controller manages to keep the rotational velocity constant by quickly adjusting the pitch angle.

5.2 Comparison with PI control

The classic proportional-integral (PI) control is a well-known and widely used scheme in the field of wind energy system, due to its simple structure and design. In this section, a comparison between the PI and ISMC control scheme is conducted and evaluated. The controller gains for the PI controller is shown in table 5.1 and is found by using the pole placement method. In appendix A.5 and A.6 the Simulink model and the MATLAB code for the PI control scheme can be found.

Table 5.1: Control gains for the PI controller

Control parameters	
Proportional gain, K_p	21.9
Integral gain, K_i	15.6

In figure 5.3 the simulation results for both the ISMC and PI control scheme are shown using the wind data from figure 5.1.

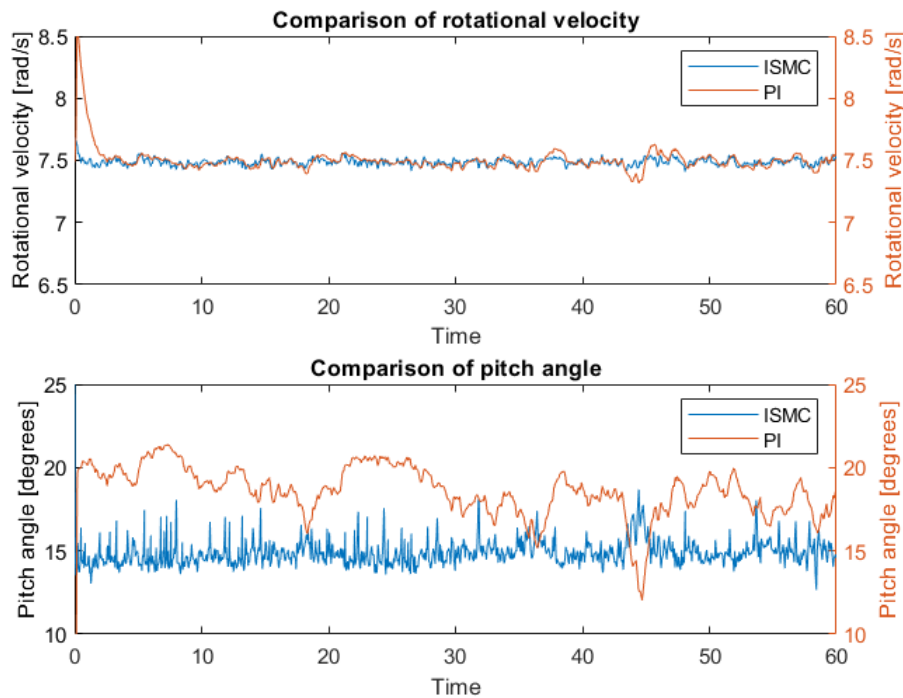


Figure 5.3: Comparison of the ISMC control scheme and the PI control scheme

The simulation shown in figure 5.3 shows that in terms of keeping the rotational velocity constant, both controller are able to do so. The controllers show that they

are very good at tracking change in the wind speed, and rapidly change pitch angle accordingly. Examining the pitch angles it is apparent that the ISMC scheme seems to have some oscillations, possibly chattering. Even though the ISMC scheme still are able maintain the rotational velocity, it is something to be aware of as it might lead to saturation in the pitch actuators.

Chapter 6

Discussion

In this chapter the discoveries from the simulation results will be discussed and evaluated.

First of all, it has been proven that it is possible to design a non-linear control scheme and implement it, theoretically, for this particular wind energy system. The study shows that by using only a conventional SMC it is not possible to get around the steady state error problem, but by adding an integral action this was solved. The different simulation results showed both good tracking capabilities and quick adjusting to rapid changes by the ISMC.

In this study, the control of a various speed various pitch wind turbine is shown by using ISMC, but this is only one of many possible control techniques. Different studies have shown various ways of using the principals of SMCs, as it is a large topic in itself. One of the major drawbacks was, as mentioned, chattering. This phenomenon is especially a problem for applicable use of SMC in the real world. For future work, it is definitely recommended to further investigate.

Another recommendation for future work on this project, is the possibility of implementing an observer to estimate other states in the system, such as generator torque or the rotor acceleration since these parameters are difficult to measure. In this project, only one state was available which was the rotational velocity and an extra variable would open up for different control techniques such as higher order SMC, which is usually use to reduce chattering. Another limitation to the project was the chosen reference values. These values were not chosen based on maximum power extraction at all, but in a range with the given data from previous work done on the experimental setup, because of limited access to experimental work on the experimental setup. As was seen from the reference rotational velocity and reference wind speed, this resulted in a very low TSR which also correspond to the low power coefficient. In this project, it has not been possible to find the power coefficient for the particular wind turbine on the experimental setup, as this normally requires experimentation. The power coefficient is an unique parameter that is dif-

ferent from each wind turbine since it depends on the type of wind turbine blade. Due to the fact that this value has not been available for the modeling of system, the derived Simulink model does not give completely accurate representation of the actual experimental setup shown in chapter 1.

Another recommendation for future work on this project, is the possibility of implementing an observer to estimate other states in the system. One of those are the rotor acceleration, since it is a difficult parameter to measure. In this project, only one state was available which was the rotational velocity and an extra variable would definitely have benefited this project. Due to the limitation of the states, higher order sliding mode techniques was not possible to examine for the elimination of chattering that occurred in the simulations.

Chapter 7

Conclusion

The objective of this study has been the design of a SMC based pitch controller operating above the rated wind speed using non-linear control scheme. Two non-linear control schemes have been proposed in this study, the conventional SMC and ISMC. The ISMC showed better performance in terms of maintaining the rotational velocity in region III control and dealing with steady state error.

In addition to the design of the controllers, the dynamic equation involving a wind energy system has been derived and a Simulink model of the system has been developed. In this study it has been shown how the steady state error problem in a various speed various pitch wind turbine can be avoided by adding an integral term to the conventional SMC. In the simulations of the control scheme, it has been proven that it is capable of adjusting to rapid changing wind speed and conduct stable reference tracking. Finally, the proposed control scheme was compared to a traditional PI control scheme which showed similar results to the ISMC. Each control method have their pros and cons, for simple non-complex system PI control might be the better option, as its design and structure are more simple and easy to use. For complex system with a lot of model uncertainties and external disturbances, SMC is the better choice, as it is more robust and capable of dealing with these parameters.

Bibliography

- [1] L. Colombo et al. *Pitch angle control of a wind turbine operating above the rated wind speed: A sliding mode control approach*. Tech. rep. Universita di Camerino and Universita Politecnica delle Marche, 2019.
- [2] Wang Xin et al. *Sliding Mode Control of Pitch Angle for direct drive PM Wind Turbine*. Tech. rep. Hunan University of Technology, 2014.
- [3] Sung-Hung Lee et al. *Sliding mode controller for torque and pitch control of wind power system based on PMSG*. Tech. rep. ASRI, School of Electrical Engineering, Seoul National University, 2010.
- [4] Jesper K. Jensen et al. *Aero-Hydro-Servo-Elastic Modelling and Control of a Scaled Floating Offshore Wind Turbine on a Tension Leg Platform Including Experimental Validation*. Tech. rep. Aalborg University Esbjerg, 2018.
- [5] Jesper K. Jensen et al. *Wind Turbine Design Modelling and Control of a Scaled Floating Offshore Tension Leg Platform*. Tech. rep. Aalborg University Esbjerg, 2017.
- [6] Maria A. B. Joergensen et al. *Individual design and implementation of torque- and collective pitch controllers for a wind turbine*. Tech. rep. Aalborg University Esbjerg, 2018.
- [7] Fernando D. Bianchi, Hernan De Battista, and Ricardo J. Mantz. *Wind Turbine Control Systems*. Springer, 2007.
- [8] Herbertt Sira-Ramirez. *Sliding Mode Control - The Delta-Sigma Modulation Approach*. Birkhauser, 2015.
- [9] Inseok Yang, Dongik Lee, and Dong Seog Han. "Designing a Robust Non-linear Dynamic Inversion Controller for Spacecraft Formation Flying". In: *Hindawi Publishing Corporation* (17 July 2014).
- [10] Ogbedeide Imahe. "From Differential equations through Lyapunov Functions to Sliding Mode Control". In: (2015, October 14).
- [11] M. Sami Fadali. *SLIDING-MODE CONTROL*. Tech. rep. Accessed May 2020. University of Nevada, Reno.

- [12] Marwa Ayadi, Fatma Ben Salem, and Nabil Derbel. *Sliding mode approach for blade pitch angle control wind turbine using PMSG under DTC*. Tech. rep. University of Sfax, December 2015.
- [13] Maria A. B. Joergensen, Thomas Hansen, and Van Roy Tran. *Design and Implementation of scaled wind turbine blades using Blade Element Momentum method and active rectifier for torque control*. Tech. rep. Aalborg University Esbjerg, 2019.
- [14] Mohsen N. Soltani et al. *Estimation of Rotor Effective Wind Speed: A Comparison*. Tech. rep. IEEE Transactions on Control System Technology, 2013.
- [15] Maria A. B. Joergensen et al. *Design and simulation of a collective pitch controller for a wind turbine*. Tech. rep. Aalborg University Esbjerg, 2017.

Appendix A

Appendix

A.1 MATLAB SMC Code

```

function [u,s] = smc(windspeed,e,omega)
%Control parameters:
K = 75;           % Control gain
psi = 1;         % Boundary layer thickness

% Parameters:
beta_ref = 15.25;
omega_ref = 7.4875;
windspeed_ref = 7;
B_m = -0.307364154597401; % B matrix
A_m = -1.20244007693585; % A matrix
E_m = 2.548991844582695; % E matrix

% Sliding Mode Control :
s = e % sliding surface

% Saturation function:
if (abs(s) > psi)
    sat_s = sign(s);
else
    sat_s = s/psi;
end

% control law:
u = beta_ref - B_m^-1*(A_m * omega - omega_ref) + E_m * ...
    (windspeed - windspeed_ref)) - (K * sat_s);
end

```

A.2 MATLAB ISMC Code

```

function [u,s] = smc(windspeed,e,int_error,omega)
    %Control parameters:
    K = 75;                % Control gain
    psi = 1;              % Boundary layer thickness
    K_ii = 6;            % ISMC integral control gain

    % Parameters:
    % beta_ref = 15.25;
    % B_m = -0.307364154597401; % B matrix
    % A_m = -1.20244007693585; % A matrix
    % E_m = 2.548991844582695; % E matrix

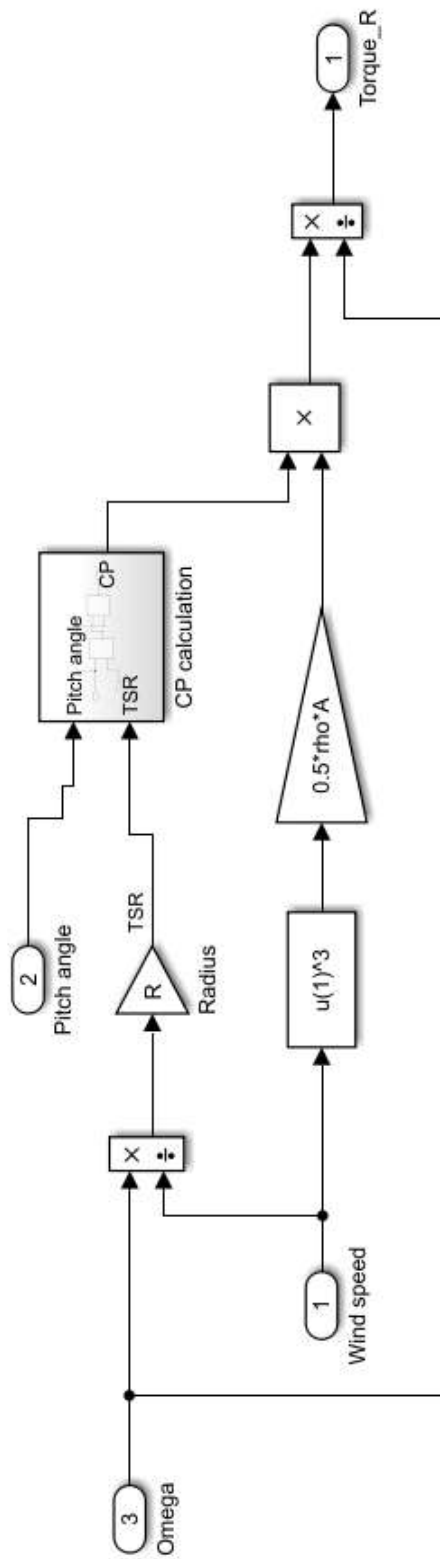
    % Sliding Mode Control :
    s = e + K_ii + int_error % sliding surface

    % Saturation function:
    if (abs(s) > psi)
        sat_s = sign(s);
    else
        sat_s = s/psi;
    end

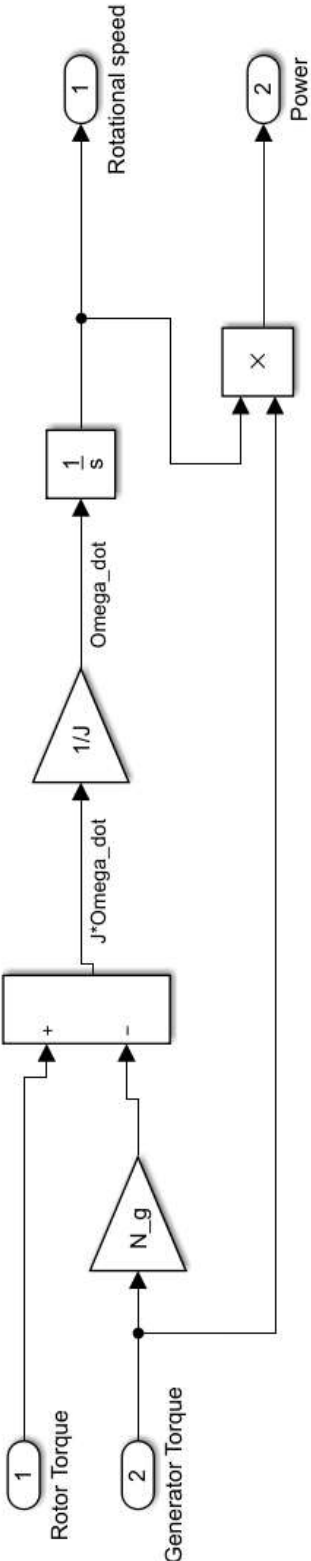
    % control law:
    u = beta_ref - B_m^-1*(A_m * omega - omega_ref) + E_m * ...
        (windspeed - windspeed_ref))) + (K_ii * e) - (K * sat_s);
end

```

A.3 Non-linear subsystem:Rotor model



A.4 Non-linear subsystem: Drive-train model



A.5 MATLAB PI Code

```
%% PI gain determination
% Pole placement
A_bar = [A_m 0; 0 C_m];
B_bar = [B_m; 0];
C_bar = [C_m 0];
D_bar = 0;

p = [-1.5, -4.5];

K = acker(A_bar,B_bar,p);
K_i = [K(1)]
K_p = [K(2)]
```

A.6 Non-linear system with PI control scheme

